



# Cloud drifts over eroding surfaces in magnetic field configurations with three field components

P. Lalousis<sup>a,\*</sup>, R. Schneider<sup>b</sup>, L.L. Lengyel<sup>b</sup>

<sup>a</sup> *Institute of Electronic Structure and Laser, Foundation for Research and Technology-HELLAS, P.O. Box 1527, Vassilika Vouten Heraklion, 71110 Crete, Greece*

<sup>b</sup> *Max-Planck-Institut für Plasmaphysik, Euratom Association, D-85748 Garching, Germany*

## Abstract

Recently a two-dimensional code (P. Lalousis, L.L. Lengyel, Nucl. Fus. 40 (2000) 1511) has been developed for calculating the time evolution of radiating vapour clouds formed over ablating solid surfaces subjected to magnetically confined energetic plasma particles. This model has now been extended to consider the effects of magnetic fields with three components. Results of comparative calculations pertaining to the erosion rates of the base plates and other characteristics are presented for three different approximations. The computational results presented show that the shielding characteristics of the evolving vapour layer are influenced by: the  $\mathbf{E} \times \mathbf{B}$ -type drift, and how the magnetic field lines are inclined with respect to the drift side. © 2001 Published by Elsevier Science B.V.

*Keywords:* 2D model; Plasma–material interaction; Electric field

## 1. Description

Recently a two-dimensional code [1] has been developed for calculating the time evolution of radiating vapour clouds formed over ablating solid surfaces (graphite divertor plates) subjected to magnetically confined energetic plasma particles. The energy carriers primarily responsible for solid surface erosion are charged particles originating from the bulk plasma and moving along the magnetic field lines. The incident electrons and ions of the disrupting plasma were assumed to be of initially Maxwellian energy distribution. They penetrate the evolving cloud along the magnetic field lines within a strip defined by the SOL width. Outside the SOL, vacuum conditions were assumed to exist at time  $t = 0$ . The magnetic field configuration was assumed to be  $\mathbf{B} = (0, B_y, B_z)$ , where  $B_y = |\mathbf{B}| \sin(\alpha)$ ,  $B_z = |\mathbf{B}| \cos(\alpha)$  and  $\alpha$  was a given angle of incidence of the grazing magnetic field. The expansion dynamics of the cloud was described in the usual continuum MHD

approximation by means of a single-fluid single-temperature model with three velocity components and with allowance for seven different species corresponding to the different ionization states of carbon. The electric field and current distributions were determined self-consistently on the basis of a properly posed boundary value problem. Heat conduction in the solid was also taken into account. The evaporation rate of the solid surface is a function of the energy flux balance at the solid and can be determined as a function of the difference between the saturated vapour pressure corresponding to the surface temperature and the actual local vapour pressure. In the present work, because of computational convenience, a rather simple expression proposed by Anisimov [2] and corresponding to evaporation in vacuum with recondensation taken into account was used. The resulting ablation rates are somewhat higher than those corresponding to real scenarios. Evaporation of carbon under  $T_s = 1300$  K was ignored.

The two-dimensional model described [1] has now been extended to consider the effects of magnetic fields with three components. Cartesian geometry is being considered, the  $x$ ,  $y$  and  $z$  coordinates correspond to the radial, vertical and toroidal directions, respectively, i.e. the base plate (divertor plate) is represented by the  $y = 0$

\* Corresponding author. Tel.: +30-81 391 827; fax: +30-81 391 305.

*E-mail address:* lalousis@iesl.forth.gr (P. Lalousis).

plane, and the poloidal plane is represented by the  $x, y$  plane. The magnetic field is given in terms of the direction cosines:  $\mathbf{B} = (B_x, B_y, B_z)$ , where  $B_x = |\mathbf{B}|\cos(\alpha)$ ,  $B_y = |\mathbf{B}|\cos(\beta)$ ,  $B_z = |\mathbf{B}|\cos(\delta)$ . The angle  $\alpha$  being the angle between the  $\mathbf{B}$  vector and the positive  $x$ -axis, and so on. The heat deposition channel from the disrupting plasma is no longer normal to the  $y = 0$  plane, it is now traced along the three dimensional magnetic field lines by appropriate stopping length calculations by taking

the effect of the induced electrostatic fields into account in a self-consistent way.

**2. Results**

In the subject scenario calculations, a carbon plate occupying the space  $y \leq 0$  is subjected to the action of plasma particles stemming from a disrupting plasma and confined to an infinite strip  $z \leq \pm \infty$  of given width in the lateral direction:  $3.5 \leq x \text{ (cm)} \leq 4.5$ . Within this strip, the plate is assumed to be an electrical conductor

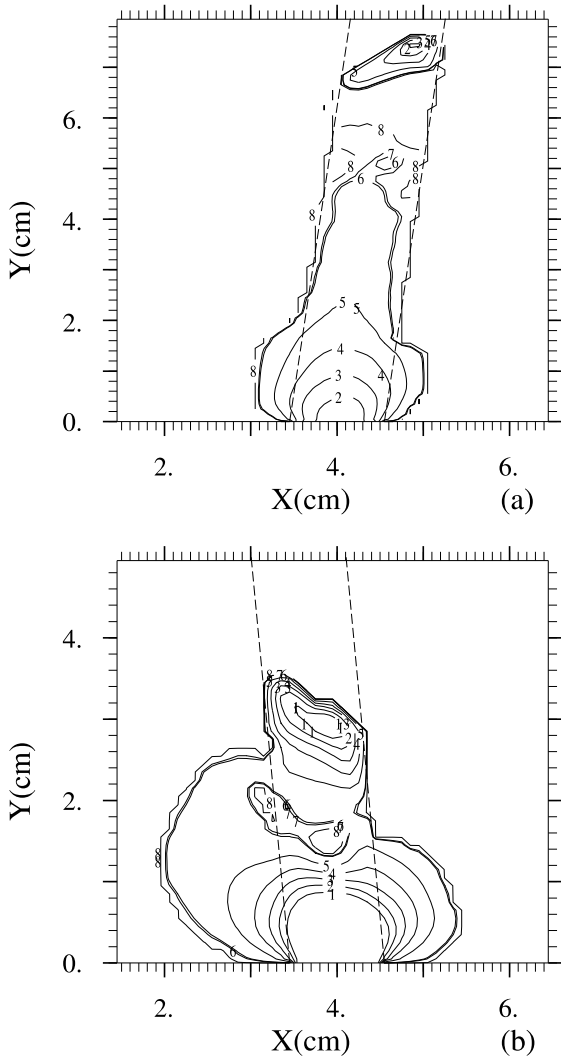


Fig. 1. Current streamline patterns in the vapour cloud at  $t = 5 \mu\text{s}$  after plasma-wall contact, for the cases (a)  $B_x = B_y$ , and (b)  $B_x = -B_y$ . Total current per unit length in the  $z$ -direction flowing between two adjacent streamlines:  $\Delta\gamma = 50 \text{ kA m}^{-1}$ . The vapour boundary approximately coincides with the streamline enveloping the current-carrying region shown. The two parallel dotted lines represent the projection of the heat deposition channel, the magnetic field lines being parallel to this channel.

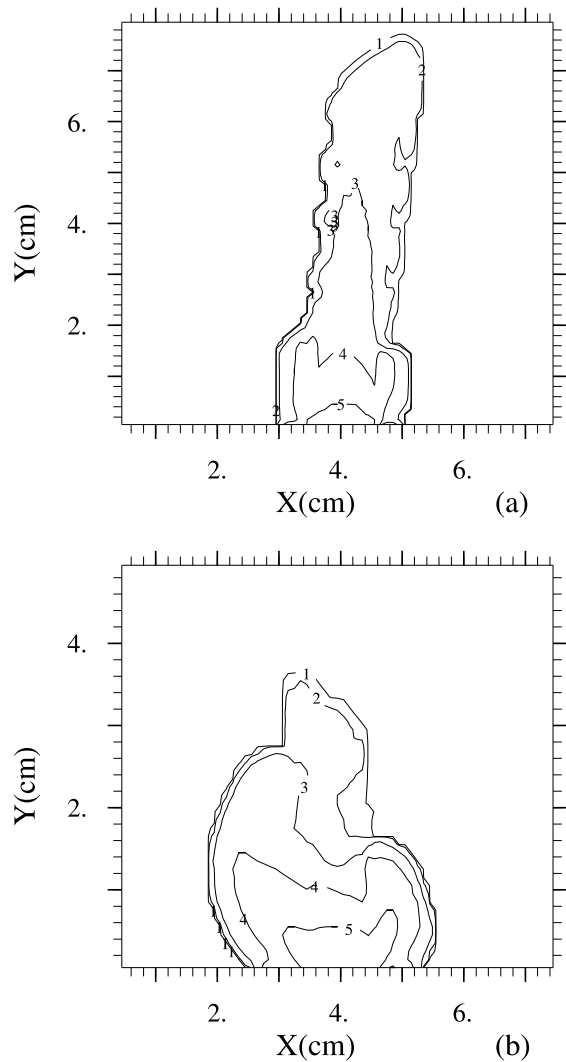


Fig. 2. Heavy particle (ions plus neutrals) density distributions in the vapour cloud at  $t = 5 \mu\text{s}$ , for (a)  $B_x = B_y$  and (b)  $B_x = -B_y$ , scenarios. Isoheight lines 1–5 correspond to heavy particle density values of  $10^{21}$ ,  $10^{22}$ ,  $10^{23}$ ,  $5 \times 10^{23}$  and  $10^{24} \text{ m}^{-3}$ , respectively.

(due to the high temperatures evolving) and an insulator outside the strip. The disrupting plasma particles are of Maxwellian energy distribution,  $T_{e0} = T_{i0} = 5$  keV,  $n_{e0} = n_{i0} = 10^{20} \text{ m}^{-3}$ , and uniform along the width of the strip. Magnetic field strength:  $|\mathbf{B}| = 6$  T. Numerical calculations were performed for the following set of direction angle values:

- (a)  $\alpha = 85.0^\circ$ ,  $\beta = 85.0^\circ$ ,  $\delta = 7.0^\circ$  ( $B_x = B_y$ ),
- (b)  $\alpha = 95.0^\circ$ ,  $\beta = 85.0^\circ$ ,  $\delta = 7.0^\circ$  ( $B_x = -B_y$ )
- (c)  $\alpha = 90.0^\circ$ ,  $\beta = 85.0^\circ$ ,  $\delta = 0.0^\circ$  ( $B_x = 0$ ).

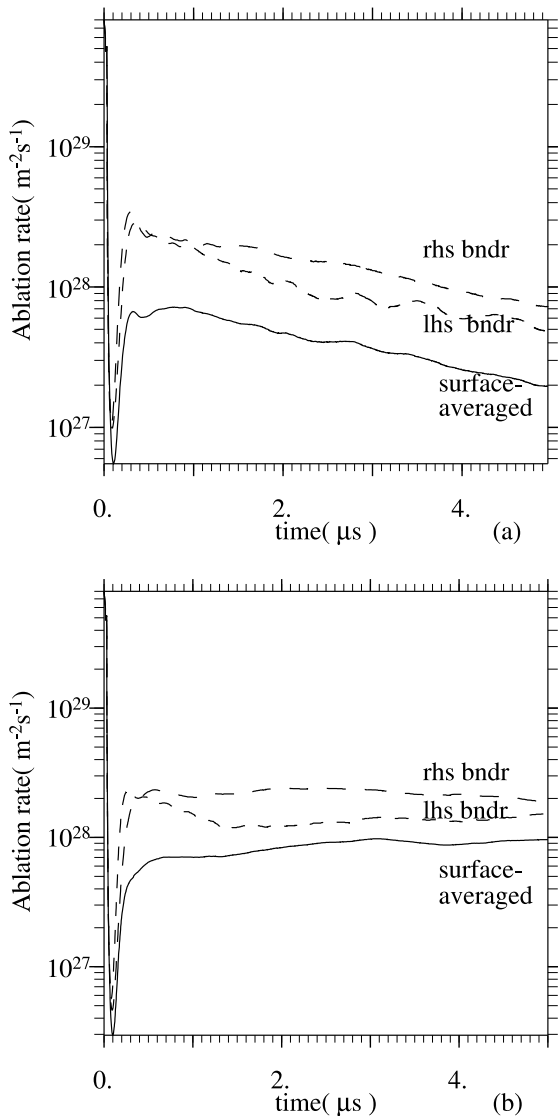


Fig. 3. Time variation of the base plate erosion rate, for (a)  $B_x = B_y$ , and (b)  $B_x = -B_y$ . Broken lines: erosion rates at the left and right edges of the conductor segment. Solid line: surface-averaged value of the erosion rate. Total number of particles eroded in 5  $\mu\text{s}$  over an area of  $0.01 \text{ m}^2$  for (a) is  $3.22 \times 10^{20}$  and for (b)  $4.8 \times 10^{20}$ .

In the scenarios (a) and (b), the field lines are not parallel to any of the three planes of the Cartesian coordinate system used. The angle between the plane  $y = 0$  (the solid plate) and the magnetic field lines is of course 5.0 degrees for all three scenarios.

Fig. 1 shows current streamline patterns monitored at  $t = 5 \mu\text{s}$  after plasma-wall contact, for magnetic configurations (a)  $B_x = B_y$ , and (b)  $B_x = -B_y$ . The streamlines are separated by equal increments of the total current:  $\Delta\gamma = 50 \text{ kA m}^{-1}$  (current per unit length in the  $z$ -direction). The maximum  $\gamma$  (current density stream function) values monitored at 5  $\mu\text{s}$  for scenarios (a) and (b) are 230 and 560  $\text{kA m}^{-1}$ , respectively.

Fig. 2 displays the heavy (ions plus neutrals) particle density contours at 5  $\mu\text{s}$ , again for magnetic configurations (a)  $B_x = B_y$ , and (b)  $B_x = -B_y$ . It is clearly seen from Fig. 1 that the ionized fraction of the vapor is confined to the magnetic field lines: the width of this cloud section (measured in the  $x$ -direction) being given roughly by the width of the 'beam plasma' strip incident at the surface. A distinct shift of the plasma column in the  $-x$ -direction can be observed in Fig. 1(b) at all time levels. The shift is related to the evolution of an  $E_\perp$  field component associated with the  $j_{y\Sigma} = 0$  boundary condition imposed at insulator surface segments. This is an  $\mathbf{E} \times \mathbf{B}$ -type drift whose origin was discussed in detail in the framework of a one-dimensional analysis [3].

The vapour boundary approximately coincides with the streamline enveloping the current-carrying region shown. The cloud height, in the  $y$ -direction, is by about

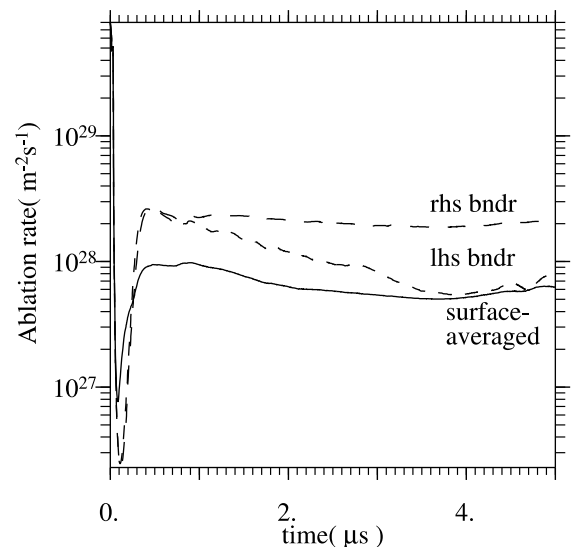


Fig. 4. Time variation of the base plate erosion rate, for the case  $B_x = 0$ . Broken lines: erosion rates at the left and right edges of the conductor segment. Solid line: surface-averaged value of the erosion rate. The total number of particles eroded in 5  $\mu\text{s}$  over an area of  $0.01 \text{ m}^2$  is  $4.24 \times 10^{20}$ .

factor of 2 larger for magnetic configuration (a) compared to magnetic configuration (b). The cloud width, in the  $x$ -direction, is by about factor of 2 larger for magnetic configuration (b) compared to magnetic configuration (a). The asymmetry in both the current streamline pattern and the heavy particle density is clearly seen in Figs. 1 and 2. It is more pronounced in scenario (b) where  $B_x = -B_y$ .

The time variation of the erosion rates, for the three scenarios, are displayed in Figs. 3 and 4. The three curves, for each scenario, correspond to the left and right edges of the heated strip and the surface-averaged value taken over the heated surface. It is shown that for this time duration the erosion rate at the right hand side of the metallic surface is larger than the erosion rate at the left-hand-side of the metallic strip, for all three different magnetic field configurations. The surface-averaged erosion rate corresponding to case (a) displays a decreasing tendency in the first 5  $\mu\text{s}$ .

### 3. Summary

In summary, results of computations based on self-consistent modelling of electrostatic phenomena [1]

show that the effect of the  $\mathbf{E} \times \mathbf{B}$  drift is more pronounced for magnetic field configurations in which the magnetic field lines are inclined towards the drift side (i.e. the LHS boundary of the strip in the above scenarios, see case (b)), than for magnetic field scenarios in which the the magnetic field lines are inclined toward the anti-drift side (i.e. the RHS boundary, see case (a)). In the case (b), the shielding characteristics are far more impaired than in the case (a), hence more intense local erosion results. When the field lines are inclined in the direction of the anti-drift side, case (a), the erosion rate of the plate is smaller. This result may be of relevance for the engineering layout of the divertor components. Reliable computational models should include electrostatic shielding effects.

### References

- [1] P. Lalouis, L.L. Lengyel, Nucl. Fus. 40 (2000) 1511.
- [2] S.I. Anisimov, V.A. Khokhlov, Instabilities in Laser-Matter Interaction, CRC, Boca Raton, FL, 1995 [Chapter 3].
- [3] L.L. Lengyel, V.A. Rozhansky, I.Yu. Veselova, P. Lalouis, Nucl. Fus. 37 (1997) 1245.